MNE 19 (2023) 100198

Contents lists available at ScienceDirect

Micro and Nano Engineering

journal homepage: www.sciencedirect.com/journal/micro-and-nano-engineering

AlGaN/GaN heterostructure based 3-dimensional force sensors

Péter Lajos Neumann [a,b,*], János Radó [a], János Márk Bozorádi [a], János Volk [a]

[a] Centre for Energy Research, Institute for Technical Physics and Materials Science, Budapest 1121, Hungary
[b] Budapest University of Technology and Economics, Department of Electron Devices, Budapest 1111, Hungary

ARTICLE INFO

Keywords:
3D force sensor
MEMS
2DEG
Strain transduction
Extreme environment
High-temperature sensor
Tactile sensing

ABSTRACT

Tactile sensing is an essential physical-electrical gateway in sensing technology. Creating such sensors is a complex challenge if the goal is to reproduce human-like sensation. Classical MEMS tactile sensor solutions in typical environmental conditions exist few types, but harsh conditions such as space technology or high-temperature range are not solved yet. One proposed material complex is the GaN/AlGaN system. In this study, we present an AlGaN/GaN MEMS force sensor for external force and load direction sensing in the mN range. The demonstrated sensor showed a sensitivity of 100 mV/N/V, which is an order of magnitude higher than the Si-based sensor with the same geometry. The sensing mechanism is based on the interface discontinuity between compound alloy layers, where two-dimensional electron gas (2DEG) is created and in which the carrier concentration can be linearly modulated by the internal crystal stress. The location of the sensing element was optimized by FEM simulation. The maximum load force of the samples varies with direction, which information allows the sensor to be used without fatigue and to obtain safety an electrical response signal under different external tensions. In addition to the advantage of this design for harsh environments, it is also possible to monolithically integrate active elements adjacent to the sensor for local acquisition and processing of the measured signal.

1. Introduction

Today, a key point in the era of an autonomous smart system is the detection and control of environmental parameters. In normal environmental conditions, the variety of employable sensing mechanisms covers almost all physical and chemical quantities. One intensively researched area is the force sensors. The micro- and nanotechnology result allows to decrease the sensitivity of force sensors down to the micro, nano and pico Newton range. That measurement system is suitable to extend atomic force measurement techniques, the study of micromechanical material properties such as hardness and modulus, fatigue and fracture of thin films, adhesion of ultra-thin films and measurement of covalent bond forces [1,2]. In autonomous systems, tactile sensing is an attractive function with many challenges [3,4], and is used as the main feedback signal of a robot arm during dexterous manipulation or invasive surgery [5,6]. The solutions that mimic natural human-like behaviours have several criteria, as collected by Z. Kappassov et al. [7], such as spatial resolution, sensitivity, frequency response, and hysteresis. Most critical applications handle fragile or soft objects that require high resolution and hysteresis-free fast response [8,9]. The operation principle of the wide variety of force sensors is based on piezoelectric [10], magnetic [11], and capacitive [12,13] sensing mechanisms. However, most of the developed sensors cannot operate out of normal environmental conditions, such as high temperatures and harsh environments. The applicability of Si- or polymer-based tactile sensors in aeronautics and space technology is limited because of their temperature degradations [14]. One prominent material candidate can be the compound alloy semiconductors to fulfil that critical environment requirement.

GaN, as a piezoelectric wide-bandgap semiconductor, can play an important role in next-generation micro- and nanoelectromechanical systems (MEMS, NEMS). It is mechanically, chemically, and electrically more resistant in harsh environments and against ionising radiation than Si, which triggers new applications in astronautical or aviation engineering [15]. The possible application spectrum of GaN-base devices is as broad as Si-based devices, but the possible high-temperature operation allows for extending the applicability in a variety of industries that require sensing and data collection in such harsh environments. The Si-based sensors and actuators can be used up to 200 °C. In contrast, for GaN-based devices, the typical upper bound is in the range of

* Corresponding author at: Centre for Energy Research, Institute for Technical Physics and Materials Science, Budapest 1121, Hungary.
E-mail address: neumann.peter.lajos@ek-cer.hu (P.L. Neumann).

https://doi.org/10.1016/j.mne.2023.100198
Received 3 January 2023; Received in revised form 24 April 2023; Accepted 5 May 2023
Available online 6 May 2023

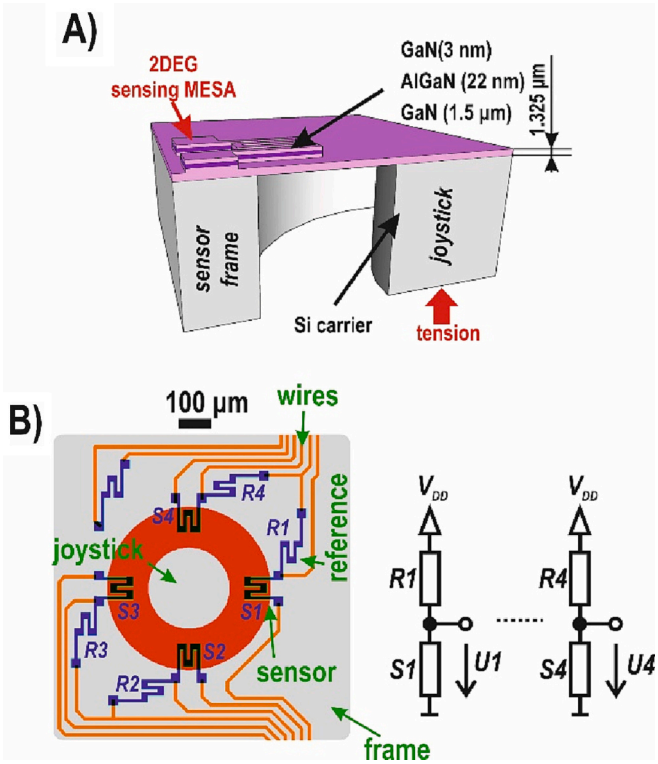

Fig. 1. The cross-section shows the quarter of the prepared MESA structure containing the 2DEG layer (A). Top view of the 2DEG force sensor with the sensor elements (S1-S4), the reference elements (R1-R4) (B) and its equivalent circuit.

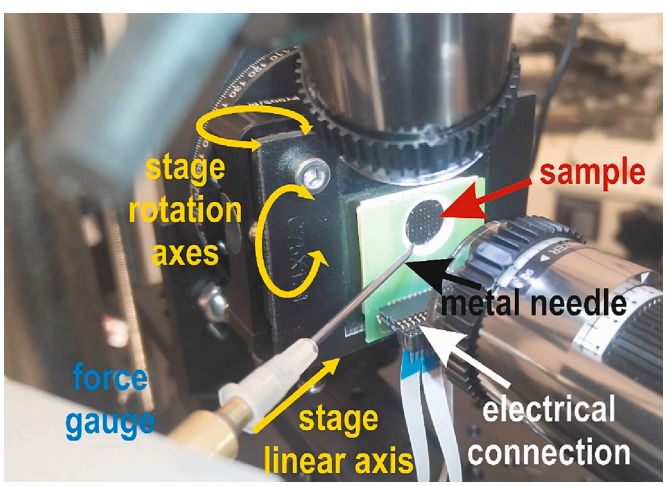

Fig. 2. Wire-bonded force sensor mounted on a three degrees of freedom vertical sample stage and loaded from the actuator side with a load cell needle and monitored by a USB camera.

600–1000 °C [16,17]. Moreover, epitaxial thin films are already commercially available on Si wafers, making them compatible with standard Si MEMS technology. Few studies introduced the heterostructure with 2DEG has exciting properties as strain sensitive [18,19] and its application as a pressure sensor [20,21].

In this work, a novel AlGaN/GaN heterostructure-based 3D force sensor is proposed. The principle of operation is similar to its Si counterpart: a thin membrane is deformed upon applying a loading force on the Si micro-stick formed on the backside of the membrane. Local strains in four positions of the membrane are measured by semiconductor gauges. By collecting the electrical signals, both the magnitude and the direction of the force can be determined. However, in contrast to conventional Si piezoresistive devices, mechanical strain influences the density of the 2-dimensional electron-gas (2DEG) at the AlGaN/GaN interface by changing the magnitude of the discontinuity in the polarisation vector between the AlGaN barrier and GaN channel layer [22]. Chapin et al. [23] showed that external strain could be a proportional modulation factor to the density of the carrier concentration.

2. Materials and methods

2.1. Sensor design and fabrication

For a side-by-side comparison with our standard Si-based 3-dimensional (3D) piezoresistive force sensor [24,25], the same device geometry was employed for the 2DEG sensor. Common to both is that a 250 µm diameter bulk micromachined microstick is used to transfer the loading force into a 500-µm-diameter deformed circular diaphragm and to sense it through strain-sensitive resistors. In this study, the substrate was a commercial high-electron-mobility transistor (HEMT) epilayer stack (GaN(3 nm)/AlGaN (22 nm)/GaN (1.5 μm)) grown onto a 4" Si wafer (NTT-AT) (Fig. 1A). The device contains two pairs of strain-sensitive 2DEG resistors (S1–4 in Fig. 1B) positioned orthogonally to each other along *x*- and *y*-axis, close to the edge of the membrane. The exact location of the four strain-sensitive HEMT resistors was optimized by finite element analysis (FEA). The sensing elements are meander-shaped MESA structures with length, width, and depth of 200 μm, 10 μm, and approx. 200 nm, respectively. Each of the sensing meanders S1–4 on the diaphragm was connected to its reference counterpart fabricated onto the undeformed Si bulk with the same geometry (R1–4 in Fig. 1B). The MESA structure was etched back into the GaN layer by Ar^+ plasma etching (Diener Pico) through a 200 nm Al masking layer, which was subsequently removed. The ohmic metal contacts for S1–4 and R1–4 resistors were fabricated by multilayer metal deposition (Ti/Al/Ti/Au) followed by rapid thermal annealing (RTA) at 825 °C in N_2 atmosphere. The flexible membrane and the Si microstick were formed by deep reactive etching (DRIE) using C_4F_8 and SF_6 process gases (Oxford ICP 180) from the backside of the Si wafer through an Al hard mask.

Transmission line method (TLM) structure was applied [26] to assess the ohmic contact quality. To this end, parallel with the force sensor process, at first a rectangular 2DEG MESA structure was etched which was partially covered with test contact pads. The size of the rectangular contact pads was 100 × 300 µm, whereas the distances between the neighbouring pads were continuously increased from 2.5 µm up to 35 µm (Fig. 5 inset).

2.2. Measurement setup

The mechanical and electromechanical measurements were carried out using a purpose-built system with three degrees of freedom sample holder (Fig. 2). The external loading was performed with a medical needle mounted on a force gauge (Andilog Centor Easy). During the alignment and testing, the position of the force gauge and the needle was precisely controlled by translational actuators (ThorLabs) and visually monitored by a USB camera (Dino-Lite Edge). A LabView software-controlled data acquisition module (NI USB 6211 DAQ) was used to power (V_{DD}) the wire-bonded 2DEG force sensor and to collect its response signals (U_1-U_4). The signals were filtered to reduce the noise.

3. Simulation

Numerical simulation was carried out by COMSOL Finite Element Method to determine the volumetric strain map in the AlGaN/GaN membrane, which predicts the possible 2DEG modulation to sense the force strength and direction. The simulated object geometry was the same as the original design. The Si parameters were taken from the

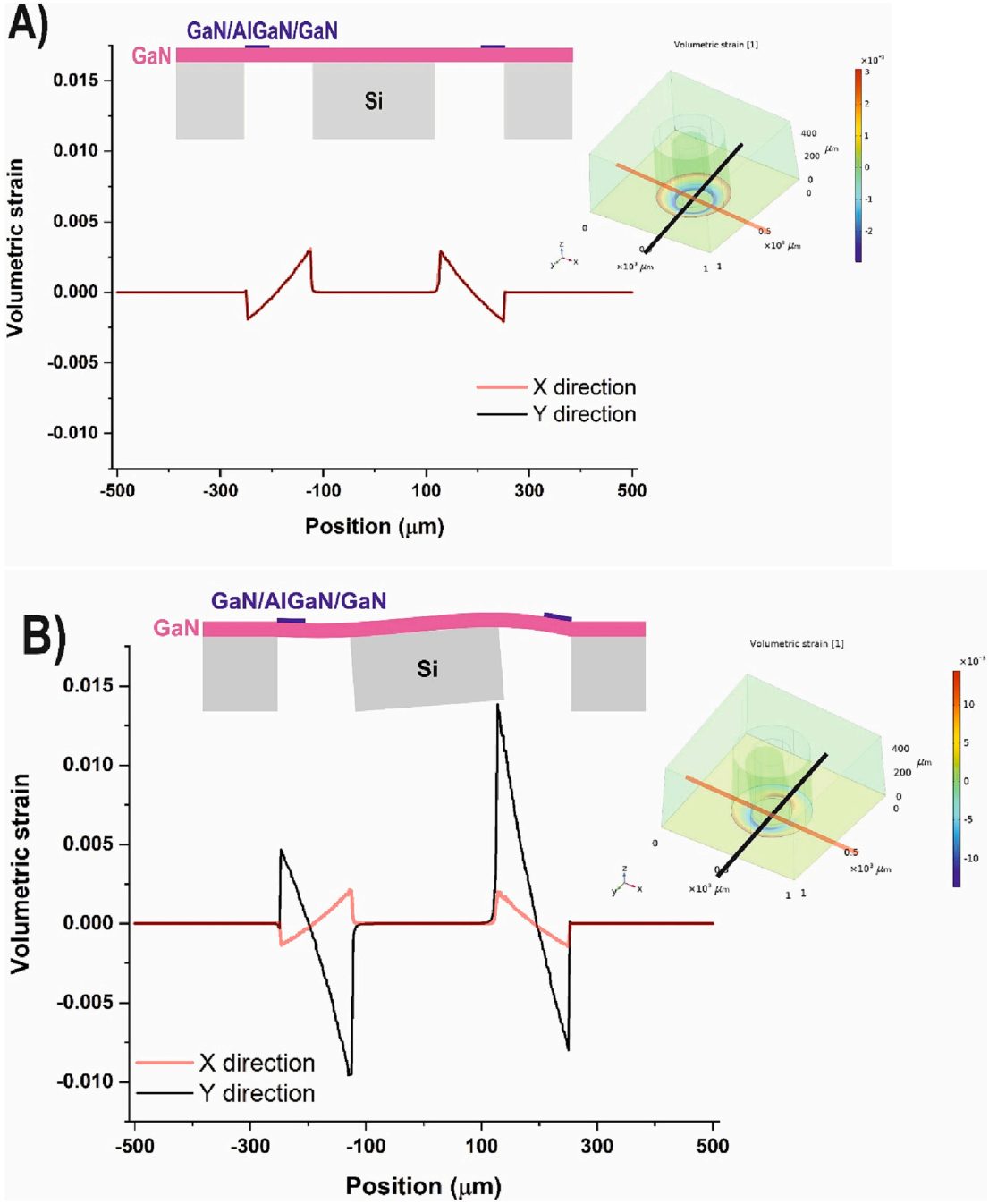

Fig. 3. Simulation results of the volumetric strain for normal ($\varphi = 0°$) (A) and oblique ($\varphi = 45°$) (B) load force, where φ is the angle with respect to the normal direction. The inset shows the simulation results of the deflection and the volumetric strain, indicating the locations of the line cuts.

COMSOL material database, except for Young's modulus of GaN, which was taken from Ref. [27] (293 GPa). In the model, the buffer layer of the compound alloy was also GaN because its material composition is unknown to customers. The Multifrontal Massively Parallel sparse direct Solver (MUMPS) was used as a stationary study solver on a fine tetrahedral meshed model. Fig. 3 shows the analytically calculated volumetric strain under an applied load of 10 mN. In normal loading direction, pointing to the centre of the Si microstick, the resulting strain is circularly symmetric and shows absolute minimum ($\varepsilon_{min} = -296$ ‰) and maximum ($\varepsilon_{max} = 311$ ‰) values close to the outer edge and to the root of the microstick, respectively (Fig. 3A). That can assume the sensor elements on the membrane will show conformity between its output signals' directions and values. In contrast, for a load force at an oblique angle $\varphi = 45°$ (where φ is the angle with respect to the normal direction), the simulation result shows a significant asymmetry of the volumetric strain building up in the membrane (Fig. 3B). The simulation results predict that there will be an asymmetric output voltage on the sensor element in the force direction and symmetrical one in the perpendicular direction, but the lower 2DEG modulation effect is due to the lower strain at the layer.

4. Results and discussion

4.1. Morphological and electrical characterisation

It was found that the III-V epilayer stack is an excellent stop layer for

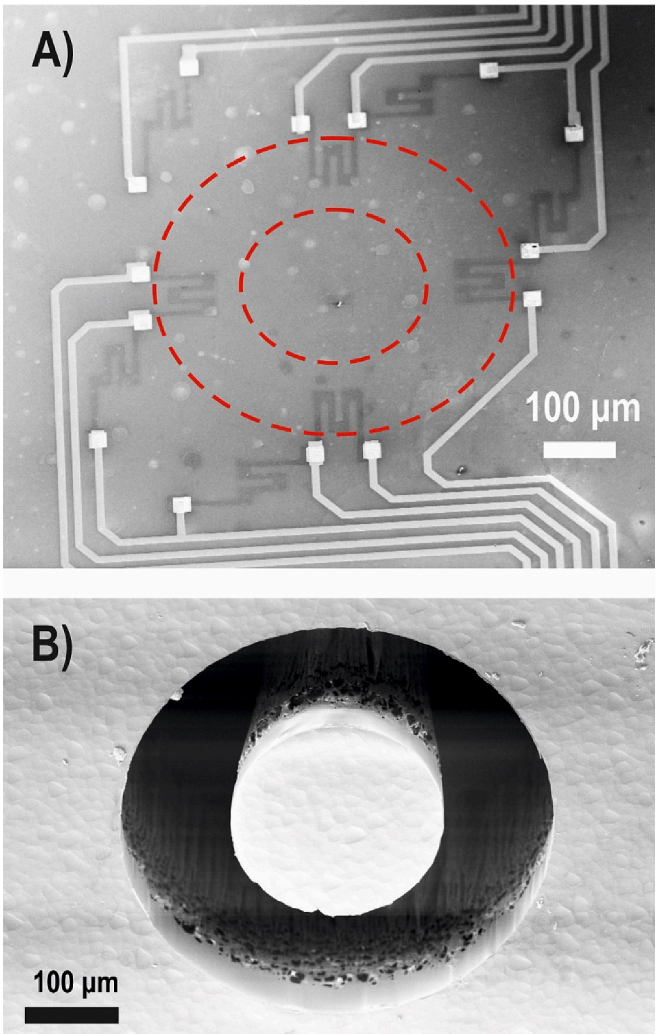

Fig. 4. SEM images of the device side (A) and joystick side (B) of the fabricated force sensor. On the device side, the red dashed lines represent the location of the joystick and membrane boundaries. (For interpretation of the references to colour in this figure legend, the reader is referred to the web version of this article.)

DRIE etching, resulting in a highly uniform and transparent diaphragm. Fig. 4A shows the structure from the device side with the S1–4 sensing and the R1–4 reference 2DEG meanders and the metal lines. The shape of the suspended Si microstick tapers from the back surface of the bulk Si towards the membrane and shows an increasing roughness in the same direction (Fig. 4B).

TLM measurement confirmed that the contacts are Ohmic, and the resistance values as a function of the interpad distance can be fitted well with a linear trendline (Fig. 5). The calculated sheet resistance is 436 Ω/sq. which is close to the nominal value obtained by Eddy's current test of the manufacturer (~460 Ω/sq). Though the specific contact resistance (8.78 10^{-5} Ωcm^2), calculated from the *y*-intersect of the TLM graph, is about one order of magnitude higher than in Ref. [28], the resulted contact resistance (~100 Ω) for the sensor elements is negligible to the total resistance of the meander circuits ($R_{SX} + R_{RX} \approx 15$ kΩ).

4.2. Fracture strength test

The characterisation of the device was started with a fracture strength test by pressing a sharp metal needle perpendicularly against the flat top surface of the Si micro-stick (Fig. 6 left). During the test, the deflection of the tip position and the applied normal force (Andilog) were recorded (Fig. 6 right). As shown in Fig. 6, all the tested GaN drumskin membranes had a reversible linear force-displacement curve, and the obtained spring constants and fracture strength are in the range of 4.2–5.3 mN/μm and 35–50 mN, respectively. The angle loaded needle measurement is required to know the maximum load force. Fig. 6 shows that the membrane fracture happened at 45° and 60° in the range of 12–26 mN and 11–12 mN, respectively. For the sensor applicability, the load force has to be below the fatigue limit by a minimum of 10%. Applied that rule of thumb, the survival rate of the sensors was 100%, which was reproduced by different sample series.

4.3. Electromechanical characterisation

The sensing MESA structures over the membrane (S1–4) and the corresponding references (R1–4) on the Si substrate holder were connected in each direction as a voltage divider to a constant bias of 1 V and measured the voltage signal on the 2DEG resistors using a fast ADC module. The applied external force changes the density of the 2DEG changes and thus the resistance of the 2-pole device. The MESA structure over the Si substrate is a fixed value resistor during the applied external force; it will not suffer any deformation, and the resistance can be used as a reference value.

In the first electromechanical experiment, the sensitivity of the force sensor on normal force load was investigated. For better visualisation, at the beginning of the measurement, a reference voltage was taken for each bridge, and only the change as a function of time upon increasing load pulses is shown in Fig. 7. All four bridges show almost the same voltage response upon increasing load. The sensitivity from the plotted curves is approx. 100 mV/N/V. This value is more than one order higher than the Si base force sensor case, where this sensitivity was approx. 9 mV/N/V [**Error! Bookmark not defined.**]. The recorded voltage signals gave a fast response (< 0.2 s) on the applied load. The response examination was followed by a dynamic normal tension analysis, in which load pulses with increasing magnitude (0–29 mN) were applied (Fig. 8). The individual sensor bridges showed increasing voltage pulses with increasing load and ran roughly together since the stress and the arising strain at the position of the symmetrically arranged MESA elements are similar.

The advantage of this geometry is that it senses the force not only in the case of perpendicular load force, but also at different angles, which allows the direction of the force to be detected. Thus, in the next experiment, the load force angle was set to $\varphi = 45°$ (Fig. 9) and increased close to the fracture strength limit of 12 mN revealed in section 4.2. It corresponds to a maximal needle deflection of approx. 950 µm. Though the U1–4 output signals are noisy, they follow the assumed trends. When the load force acts from the direction of S4, symmetrical stress surrounding the S1 and S3 MESA sensor elements appears, and the response signal has the same level and propagation. It can be assumed that the carrier density modulation in the 2DEG is the same for S1 and S3 cases. In contrast, S2 and S4 show significantly different signals due to the asymmetry in the longitudinal direction. This is because one side compressed the MESA structure, and the other was tensile. The generated strain in the layer at S2 and S4 is much higher than at S1 and S3, which results higher signal from the load direction sensor pair.

5. Conclusions

In this article was demonstrated an AlGaN/GaN MEMS force sensor which can sense the external force and deflection direction. The base of the sensing is the interface discontinuity between compound alloy layers where 2DEG was established. During the experiment, the 2DEG carrier concentration can be modulated by the crystal's internal strength linearly in the range of millinewton. The simulation tools were successfully applied to determine the sensing area, and it allowed the use of different arrangements in the next sensor development step to get more precise information about the external force characteristics. The fabrication

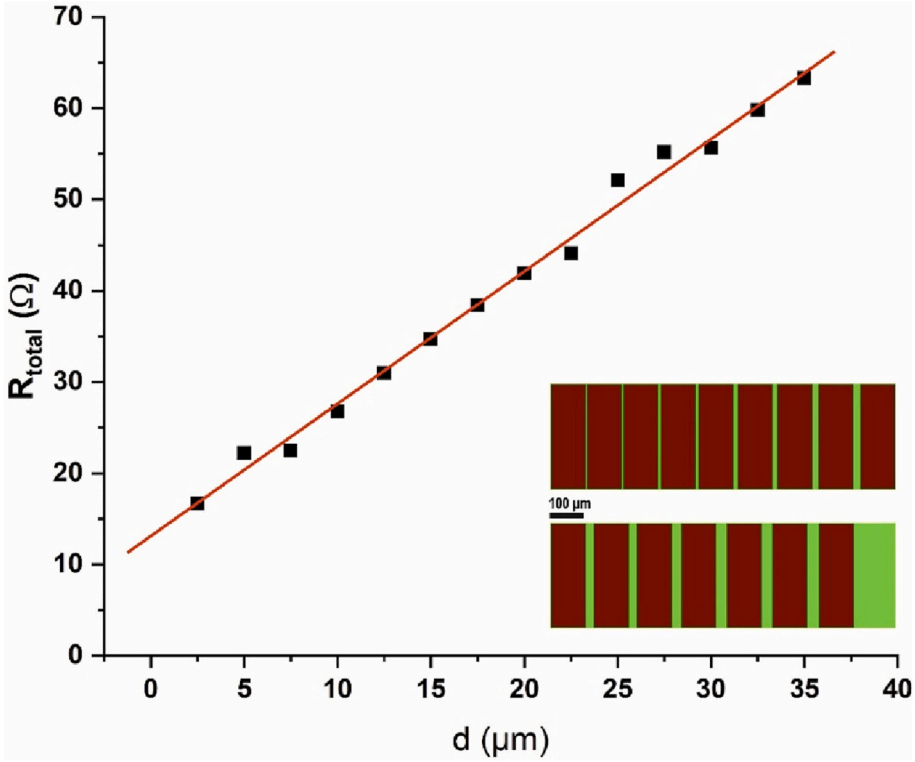

Fig. 5. Results of the transmission line method (TLM) and the design of the test (inset).

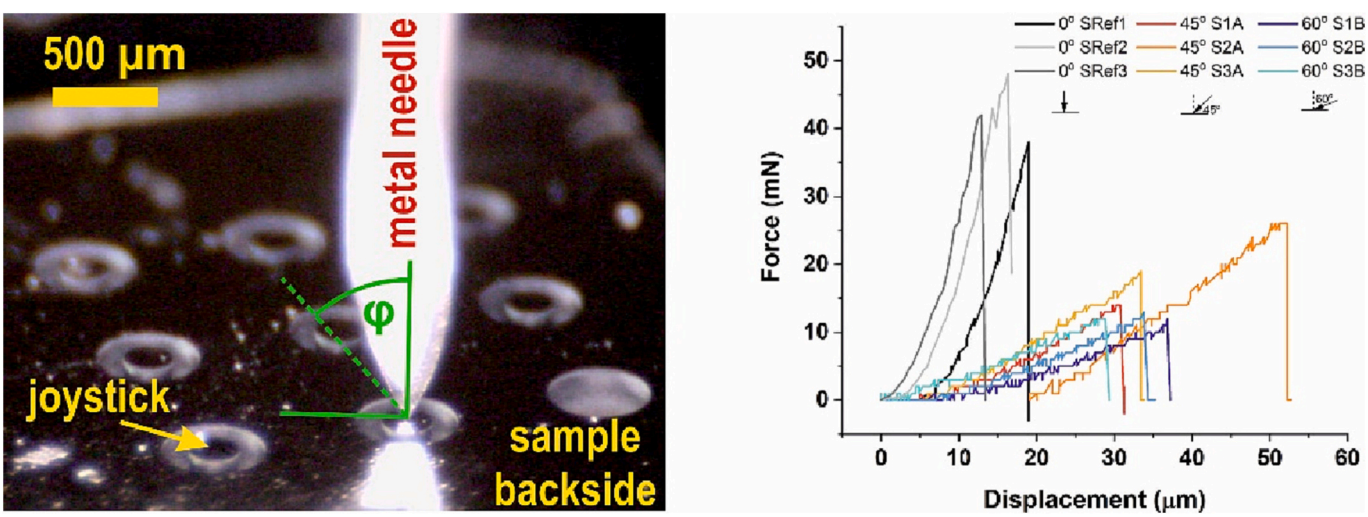

Fig. 6. Camera image of the needle tip in contact with the force sensor (left) and the measured loading force-displacement test result of nine test membranes (right).

process of the MEMS device was successful and reproducible, which allows further consideration of this concept. It is possible to monolithic integrate active elements next to the sensor to gain and process the measured signal locally [29] without any doping or special treatments. This work has many possibilities for further development, such as the carrier density depends on the compound alloy' atoms ratio, which can redefine the resistance of the same geometry to get less noise. A further plan to get an accurate tensile sensor for harsh environments is to investigate the temperature sensing and dependency, the direction decoding from the recognised response of the voltage divider, and the matrix arrangement of the sensors to obtain redundancy information for the precise touching information.

Declaration of Competing Interest

The authors declare the following financial interests/personal relationships which may be considered as potential competing interests:

Janos Volk reports financial support was provided by Ministry of Innovation and Technology of Hungary from the National Research, Development and Innovation Fund, financed under the TKP2021 funding.

Data availability

No data was used for the research described in the article.

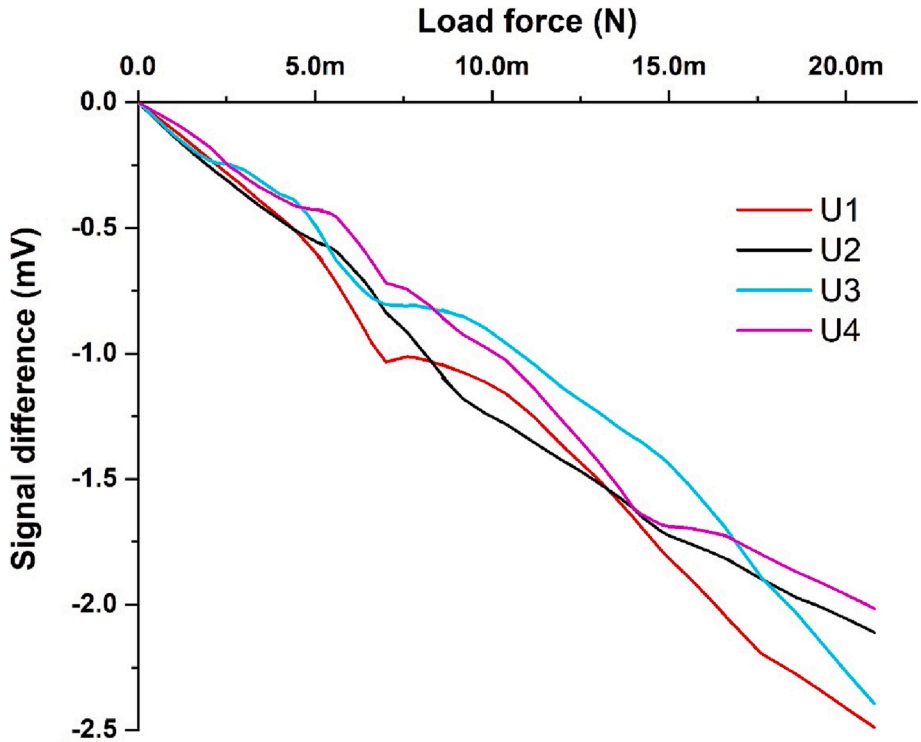

Fig. 7. Normal load force response signals of the sensor outputs.

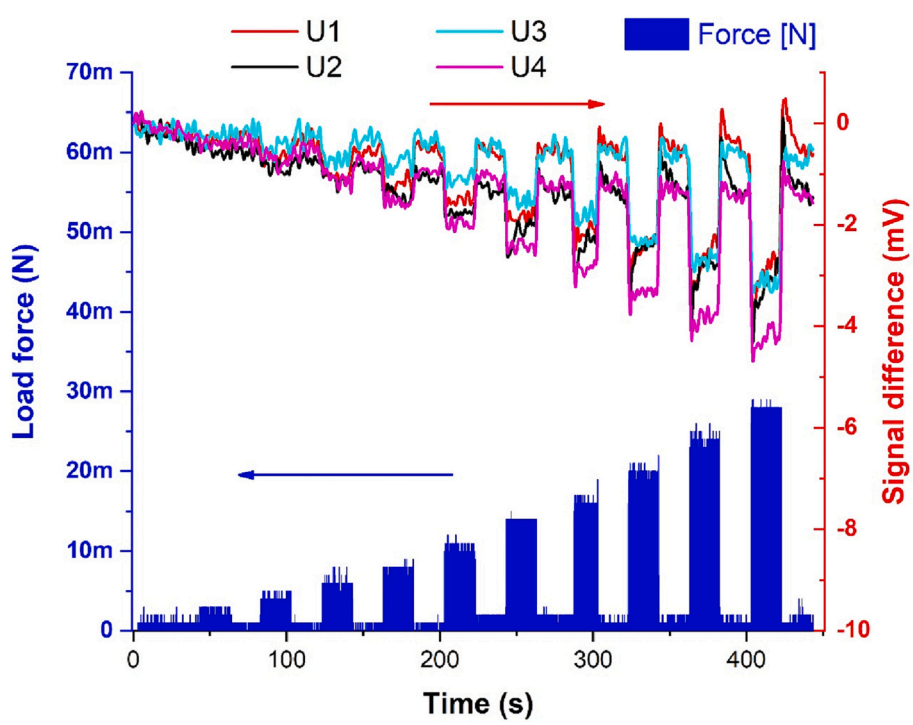

Fig. 8. Sensor output signal for increasing normal load pulses as a function of time.

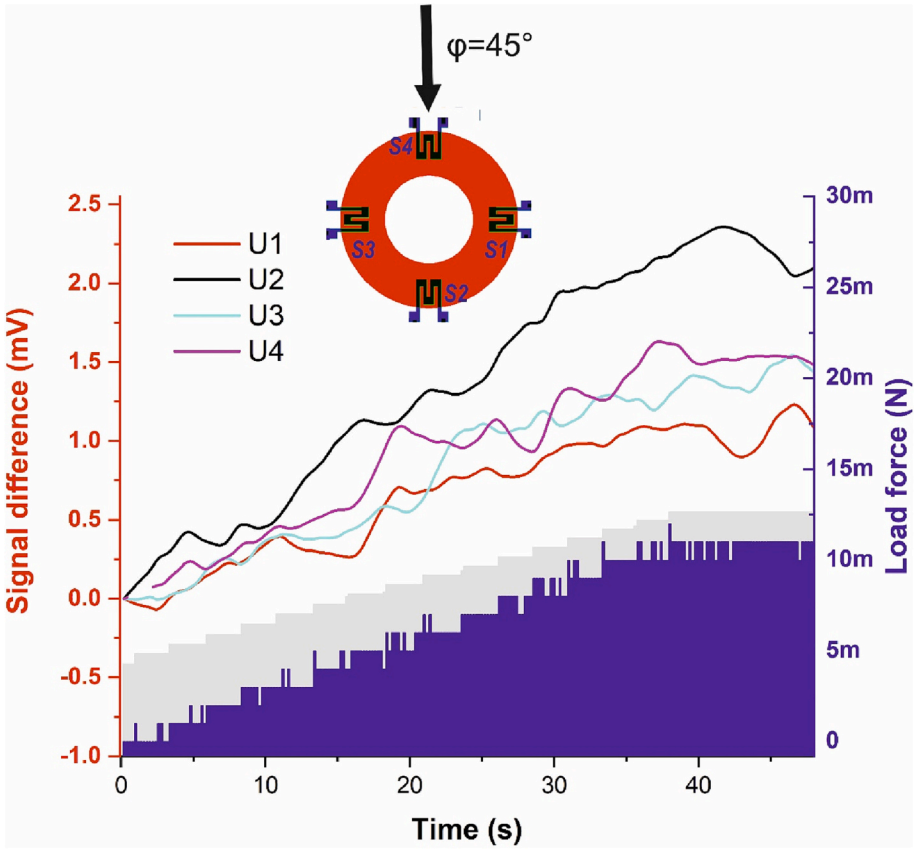

Fig. 9. Sensor output signal for increasing $\varphi = 45^\circ$ load force as a function of time. The grey region represents the needle displacement (total step length ≈ 950 μm).

Acknowledgement

Project no. TKP2021-NVA-03 has been implemented with the support provided by the Ministry of Innovation and Technology of Hungary from the National Research, Development and Innovation Fund, financed under the TKP2021 funding scheme. The authors wish to explain their gratitude to János Ferencz, Attila Nagy, Zoltán Szabó and István Endre Lukács for the sample preparation support.

References

[1] V. Nesterov, Facility and methods for the measurement of micro and nano forces in the range below 10−5 N with a resolution of 10−12 N, Meas. Sci. Technol. 18 (2007) 360.
[2] T. Hong, T. Wang, Y.Q. Xu, Direct measurement of π coupling at the single-molecule level using a carbon nanotube force sensor, Nano Lett. 18 (2018) 7883–7888.
[3] H. Mnyussiwalla, P. Seguin, P. Vulliez, J.P. Gazeau, Evaluation and selection of grasp quality criteria for dexterous manipulation, J. Intell. Robot. Syst. 104 (2022) 20, https://doi.org/10.1007/s10846-021-01554-4.
[4] I.S. Bayer, MEMS-based tactile sensors: materials, processes and applications in robotics, mems-basedtactile sensors: materials, processes and applications in robotics, Micromachines 13 (2022) 2051, https://doi.org/10.3390/mi13122051.
[5] O.S. Bholat, R.S. Haluck, R.H. Kutz, P.J. Gorman, T.M. Krummel, Defining the role of haptic feedback in minimally invasive surgery, Stud. Health Technol. Inform. 62 (1999) 62–66 (PMID: 10538400).
[6] B. Zhao, C.A. Nelson, A sensorless force-feedback system for robot-assisted laparoscopic surgery, Comp. Assis. Surg. 24 (S1) (2019) 36–43.
[7] Z. Kappassov, J.A. Corrales, V. Perdereau, Tactile sensing in dexterous robot hands, in: Robotics and Autonomous Systems 74 A, 2015, pp. 195–220, https://doi.org/10.1016/j.robot.2015.07.015.
[8] J.M. Romano, K. Hsiao, G. Niemeyer, S. Chitta, K.J. Kuchenbecker, Human-inspired robotic grasp control with tactile sensing, IEEE Trans. Robot. 27 (6) (2011) 1067–1079, https://doi.org/10.1109/TRO.2011.2162271.
[9] H. Yussof, M. Ohka, H. Suzuki, N. Morisawa, S.-I. Ao, B. Rieger, S.-S. Chen, Advances in computational algorithms and data analysis, in: Lecture Notes in Electrical Engineering vol. 14, Springer, Netherlands, 2009, pp. 199–213, https://doi.org/10.1007/978-1-4020-8919-0_15.
[10] T.C. Duc, J.F. Creemer, P.M. Sarro, Lateral nano-Newton force-sensing piezoresistive cantilever for microparticle handling, J. Micromech. Microeng. 16 (2006) S102–S106.
[11] X. Guo, W. Hong, T. Zhang, et al., Highly stretchable, responsive flexible dual-mode magnetic strain sensor, Adv. Mater. Technol. 8 (2023) 2201439.
[12] C. Mahata, H. Algadi, J. Lee, S. Kim, T. Lee, Biomimetic-inspired micro-nano hierarchical structures for capacitive pressure sensor applications, Measurement 151 (2020), 107095.
[13] Y. Zhao, X. Guo, W. Hong, et al., Biologically imitated capacitive flexible sensor with ultrahigh sensitivity and ultralow detection limit based on frog leg structure composites via 3D printing, Compos. Sci. Technol. 231 (2023), 109837.
[14] D.G. Senesky, B. Amshidi, A.P. Pisano, Harsh EnvironmentSilicon carbide sensors for health and performance monitoring of aerospace systems: a review, IEEE Sensors J. 9 (11) (2009) 1472–1478, https://doi.org/10.1109/JSEN.2009.2026996.
[15] K.T. Upadhyay, M.K. Chattopadhyay, Sensor applications based on AlGaN/GaN heterostructures, Mater. Sci. Eng. B 263 (2021), 114849, https://doi.org/10.1016/j.mseb.2020.114849.
[16] A.S. Yalamarthy, D.G. Senesky, Strain- and temperature-induced effects inAlGaN/GaN high electron mobility transistors, Semicond. Sci. Technol. 31 (2016), 035024, https://doi.org/10.1088/0268-1242/31/3/035024.
[17] D. Maier, M. Alomari, N. Grandjean, J.F. Carlin, M.A. Diforte-Poisson, C. Dua, S. Delage, E. Kohn, InAlN/GaN HEMTs for operation in the 1000°C regime: a firstexperiment, IEEE Electron Device Lett. 33 (2012) 985–987, https://doi.org/10.1109/LED.2012.2196972.
[18] S. Chu, F. Ren, S. Pearton, B. Kang, S. Kim, B. Gila, C. Abernathy, J.I. Chyi, W. Johnson, J. Lin, Piezoelectric polarization-induced two dimensional electrongases in AlGaN/GaN heteroepitaxial structures: application formicro-pressure sensors, Mater. Sci. Eng. A 409 (2005) 340–347, https://doi.org/10.1016/j.msea.2005.05.119.
[19] A.S. Yalamarthy, D.G. Senesky, Strain- and temperature-induced effects inAlGaN/GaN high electron mobility transistors, Semicond. Sci. Technol. 31 (2016) 035024, https://doi.org/10.1088/0268-1242/31/3/035024.
[20] B.S. Kang, S. Kim, F. Ren, J.W. Johnson, R.J. Therrien, P. Rajagopal, J.C. Roberts, E.L. Piner, K.J. Linthicum, S.N. Chu, K. Baik, B.P. Gila, C.R. Abernathy, S. J. Pearton, Pressure-induced changes in the conductivity of AlGaN/GaNhigh-electron mobility-transistor membranes, Appl. Phys. Lett. 85 (2004) 2962, https://doi.org/10.1063/1.1800282.
[21] E. Le Boulbar, M. Edwards, S. Vittoz, G. Vanko, K. Brinkfeldt, L. Rufer, P. Johander, T. Lalinsk'y, C. Bowen, D. Allsopp, Effect of bias conditions onpressure sensors based on AlGaN/GaN high electron mobility transistor, Sens.Actuat. A: Phys 194 (2013) 247–251, https://doi.org/10.1016/j.sna.2013.02.017.

[22] C.E.C. Wood, D. Jena, Polarization Effects in Semiconductors: From Ab Initio Theory to Device Application, Springer, New York, 2008. ISBN: 978–0–387-68319-5.
[23] C.A. Chapin, R.A. Miller, K.M. Dowling, R. Chen, D.G. Senesky, InAlN/GaN high electron mobility micro-pressure sensors forhigh-temperature environments, Sensors Actuators A 263 (2017) 216–223, https://doi.org/10.1016/j.sna.2017.06.009.
[24] D. Molnár, A. Pongrácz, M. Ádám, Z. Hajnal, V. Timárné, G. Battistig, Sensitivity tuning of a 3-axial piezoresistive force sensor, Microelectron. Eng. 90 (2012) 40–43, https://doi.org/10.1016/j.mee.2011.05.030.
[25] J. Radó, C. Dücső, P. Földesy, G. Szebényi, Z. Nawrat, K. Rohr, P. Fürjes, 3D force sensors for laparoscopic surgery tool, Microsyst. Technol. 24 (2018) 519–525, https://doi.org/10.1007/s00542-017-3443-4.
[26] T. Abbas, L. Slewa, Transmission line method (TLM) measurement of (metal/ZnS) contact resistance, Int. J. Nanoelectr. Mater. 8 (2015) 111–120.
[27] H.Y. Huang, Z.Y. Li, J.Y. Lu, Z.J. Wang, C.S. Wang, K.M. Lau, K.J. Chen, T.Y. I. Zhang, Microbridge tests on gallium nitride thin films, J. Micromech. Microeng. 19 (2009) 095019, https://doi.org/10.1088/0960-1317/19/9/095019.
[28] K. Floros, X. Li, I. Guiney, S.J. Cho, D. Hemakumara, D.J. Wallis, E. Wasige, D.A. J. Moran, C.J. Humphreys, I.G. Thayne, Dual barrier InAlN/AlGaN/GaN-on-silicon high-electron-mobility transistorswith Pt- and Ni-based gate stacks, Phys. Status Solidi A214 (8) (2017) 1600835, https://doi.org/10.1002/pssa.201600835.
[29] M.R. Zadeh, V.J. Gokhale, A. Ansari, M. Faucher, D. Theron, Y. Cordier, L. Buchaillot, Gallium nitride as an electromechanical material, J. Microelectromech. Syst 23 (2014) 1252–1271, https://doi.org/10.1109/JMEMS.2014.2352617.